

Article

Assessing Waste Marble Powder Impact on Concrete Flexural Strength Using Gaussian Process, SVM, and ANFIS

Nitisha Sharma ¹, Mohindra Singh Thakur ¹, Raj Kumar ^{2,*}, Mohammad Abdul Malik ³, Ahmad Aziz Alahmadi ⁴, Mamdooh Alwetaishi ⁵ and Ali Nasser Alzaed ⁶

¹ Department of Civil Engineering, Shoolini University, Solan 173229, Himachal Pradesh, India

² Faculty of Engineering and Technology, Shoolini University, Solan 173229, Himachal Pradesh, India

³ Engineering Management Department, College of Engineering, Prince Sultan University, Riyadh 11586, Saudi Arabia

⁴ Department of Electrical Engineering, College of Engineering, Taif University, Taif 21944, Saudi Arabia

⁵ Department of Civil Engineering, College of Engineering, Taif University, Taif 21944, Saudi Arabia

⁶ Department of Architecture Engineering, College of Engineering, Taif University, Taif 21944, Saudi Arabia

* Correspondence: raj.me@shooliniuniversity.com

Abstract: The study's goal is to assess the flexural strength of concrete that includes waste marble powder using machine learning methods, i.e., ANFIS, Support vector machines, and Gaussian processes approaches. Flexural strength has also been studied by using the most reliable approach of sensitivity analysis in order to determine the influential independent variable to predict the dependent variable. The entire dataset consists of 202 observations, of which 120 were experimental and 82 were readings from previous research projects. The dataset was then arbitrarily split into two subsets, referred to as the training dataset and the testing dataset, each of which contained a weighted percentage of the total observations (70–30). Output was concrete mix flexural strength, whereas inputs comprised cement, fine and coarse aggregates, water, waste marble powder, and curing days. Using statistical criteria, an evaluation of the efficacy of the approaches was carried out. In comparison to other algorithms, the results demonstrate that the Gaussian process technique has a lower error bandwidth, which contributes to its superior performance. The Gaussian process is capable of producing more accurate predictions of the results of an experiment due to the fact that it has a higher coefficient of correlation (0.7476), a lower mean absolute error value (1.0884), and a smaller root mean square error value (1.5621). The number of curing days was identified as a significant predictor, in addition to a number of other factors, by sensitivity analysis.

Keywords: waste marble powder; flexural strength; support vector machines; Gaussian processes; ANFIS



Citation: Sharma, N.; Thakur, M.S.; Kumar, R.; Malik, M.A.; Alahmadi, A.A.; Alwetaishi, M.; Alzaed, A.N. Assessing Waste Marble Powder Impact on Concrete Flexural Strength Using Gaussian Process, SVM, and ANFIS. *Processes* **2022**, *10*, 2745. <https://doi.org/10.3390/pr10122745>

Academic Editor: Xiong Luo

Received: 26 October 2022

Accepted: 16 December 2022

Published: 19 December 2022

Publisher's Note: MDPI stays neutral with regard to jurisdictional claims in published maps and institutional affiliations.



Copyright: © 2022 by the authors. Licensee MDPI, Basel, Switzerland. This article is an open access article distributed under the terms and conditions of the Creative Commons Attribution (CC BY) license (<https://creativecommons.org/licenses/by/4.0/>).

1. Introduction

Cement, fine and coarse aggregates and water are the main ingredients of concrete. Every one of the components, with the exception of cement, is easily accessible in every region of the world. The only way to create cement is through the process of manufacturing it. The manufacture of cement results in the emission of carbon dioxide, which is harmful to the environment. Because of their extensive application, there is currently an increase in the overexploitation of several resources. As a result of industrialization and urbanization, concrete is used in a significant amount of construction projects, and the rising demand for the material will eventually lead to its depletion. If the waste material could meet the required criteria, then it could be used in the development of the infrastructure, which would make it economically viable [1,2]. The process of industrialization results in the production of a variety of hazardous wastes, the management of which can be accomplished by mixing these wastes into the fundamental components of concrete. There is a possibility that fly ash, silica fumes, and slag will raise the water demand of the concrete mix. This issue can be remedied by using a superplasticizer [3]. Waste marble powder (WMP)

can be utilized in place of cement or fine aggregates as an alternative [4–6]. WMP is a potentially useful material that might be used to partially replace sand and cement. CaO , SiO_2 , Al_2O_3 , Fe_2O_3 are significant constituents, whereas MgO , SO_3 , K_2O , and Na_2O are minor constituents. India produces the most marble waste throughout the mining process. The marble industry's waste can harm the environment and the economy if not properly managed. The demand for marble on the market is driven in part by its widespread application in ornamental settings. The production of marble results in the generation of a number of different chemical forms that are considered to be hazardous waste. The disposal of waste is not an efficient use of resources, and it also raises concerns for the environment. When appropriately integrated, the use of waste from industrial processes has the potential to reduce the amount of cement that must be added to concrete [7]. Marble sludge can be recycled and utilized as one of the primary components of concrete mix, which can subsequently be used as a building material or in the construction of road pavements, amongst other potential applications [8]. Soliman [9] found that as marble powder (MP) replaces cement in the nominal mix, the concrete strength decreases. Both the effect of substituting MP for cement (C) and the findings show that the tensile strength of WMP starts to decrease as the amount of WMP increases [10]. By replacing 10% of the cement with marble dust, Dhoka [11] noticed a 25% improvement in 28-day tensile strength compared to the composite samples. Many researchers use waste MP as a replacement of cement by weight [12–16]. In the experiment that was carried out by Kelestemur [14], on a concrete mix that contained various amounts of glass fiber, it can be seen that by adding marble dust, it achieves the highest CS. Workability was not affected by the capillarity properties of self-compacting concrete caused by the addition of waste marble dust as a cement replacement, but tensile strength was reduced as a result [15]. Uysal and Yilmaz [17] investigated the usage of lime, basalt, and MP as Portland cement substitutes. In addition, the tensile strength after 28 days was improved when both gravel and sand were used as a substitute [18]. It was determined that the utilization of MP as a filler was satisfactory [19]. According to the findings of the study, replacing sand with 10% mineral powder delivers the highest possible CS while maintaining a level of workability that is comparable to that of cement. MP offers good cohesiveness to mortar because of its fineness. MP can also be used as a substitute for SCC [20]. After 28 days of curing, Demirel [21] found that the porosity of the matrix began to decrease as the quantity of small particles in the matrix increased after being replaced with WMP. However, the CS rating improved. The mechanical and physical qualities of the concrete are altered when WMP is used as a filler ingredient in the production of SCC [22].

Waste marble powder (WMP) can be utilized in place of cement or fine aggregates as an alternative [5,6]. Researchers are currently employing methods of soft computing in an effort to find solutions to the problems [23–32]. The amount of cement, aggregates, water, admixtures, and waste products that are included in the mix are the primary factors that define the strength of the concrete. These elements can be incorporated into the model as input variables to facilitate more accurate forecasting of the ultimate outcome. In classic methodologies, the approaches of linear and non-linear regression are utilized the majority of the time in order to anticipate results. However, in recent years, techniques from the field of AI such as artificial neural networks (ANN), linear regression, group method of data handling (GMDH), random forest, and random tree (RT) have been utilized to estimate the concrete mechanical characteristics [33–38]. The majority of the research effort is being put towards attempting to forecast the mechanical characteristics of various concrete mixes. In order to accurately estimate the strength of no-slump concrete, a number of regressions, neural networks (NNT), and adaptive neuro-fuzzy inference system (ANFIS) models have been created [25,32]. These models use components of concrete as input parameters. The findings indicate that the NNT and ANFIS models are superior to the proposed standard regression models in terms of accuracy when it comes to forecasting the 28-day CS for non-slumping concrete. In Madandoust's [39] research, a neural network of the GMDH type was combined with ANFIS modelling to make a prediction about the strength of concrete made

from cementitious components. During the course of the research, a genetic algorithm was utilized to construct a neural network of the GMDH variety. Input parameters consisted of things like ratios of length to diameter, core diameter, and other similar measurements in order to forecast the output strength. Ayat [40], in the year 2018, directed the study to analyse the affectability of the developed model to some basic factors influencing concrete CS. The goal of the investigation was to determine whether or not the constructed model is affected by these factors. It was found that the ANNs model that had been suggested was remarkable as a practical and very effective method for simulating the CS forecast of lime filler (LF) concrete. When it comes to forecasting the CS of concrete mixtures, tree-based models perform admirably.

In this paper, the effect of marble powder on flexural strength of concrete is demonstrated. Experimental investigations to study the effect of marble dust on flexural strength exploring possible reasons for the gain in strength have been conducted. Techniques from the field of soft computing have found widespread use in a variety of technical fields over the course of the past few decades. Fewer studies have been identified on the performance of soft computing techniques for predicting the FS of concrete mixtures that include waste MP. Some of the soft computing techniques that were utilized in this work are the Support Vector Machine (SVM), the Gaussian Process (GP), and the Adaptive Neuro-Fuzzy Inference System (ANFIS). The results were compared in order to identify the modelling strategy that proved to be the most reliable in predicting the FS of concrete mix includes waste marble powder. Additional sensitivity analysis was done to identify the most important input parameter.

2. Machine Learning Techniques

2.1. ANFIS

An artificial neural network that is built on the Takagi-Sugeno fuzzy inference system is called an adaptive neuro-fuzzy inference system (ANFIS). It wasn't until the early 1990s that the methodology was created. It offers the chance to use the benefits of both types of systems under a single framework because it combines neural networks and fuzzy logic concepts. Its inference system is made up of a collection of fuzzy IF-THEN rules with the capacity to approximate nonlinear functions through learning. As a result, ANFIS is regarded as a universal estimator. The best parameters acquired by genetic algorithm may be used to employ the ANFIS in a more efficient and optimal manner. Figure 1 presents the ANFIS architecture [41]. There are five layers in the ANFIS model. Each layer has its own set of nodes, which are specified by the node function. Layer one is the layer in which all of the nodes have a node function and are adaptive nodes. The second layer is where nodes multiply incoming signals, and the output is the sum of all the incoming signals. The firing strength of the *i*th rule is compared to the total firing strength of all node rules, which is the focus of Layer 3's calculation. Each node in layer 4 is responsible for calculating the contribution that the *i*th rule makes to the overall output. The signal node in layer 5 calculates the final output as the sum of all input signals.

Within the framework of this ANFIS system, the hybrid algorithm was implemented. The input and output membership functions of the ANFIS model each have their own unique shape. The 'trimf' membership function was chosen out of all the other MF's because it displays the lowest test error and the lesser value of mean absolute percentage error compared to the other membership functions. The 'trimf' membership function, which stands for 'triangular membership function,' also has incline and decline features with a specific value [42].

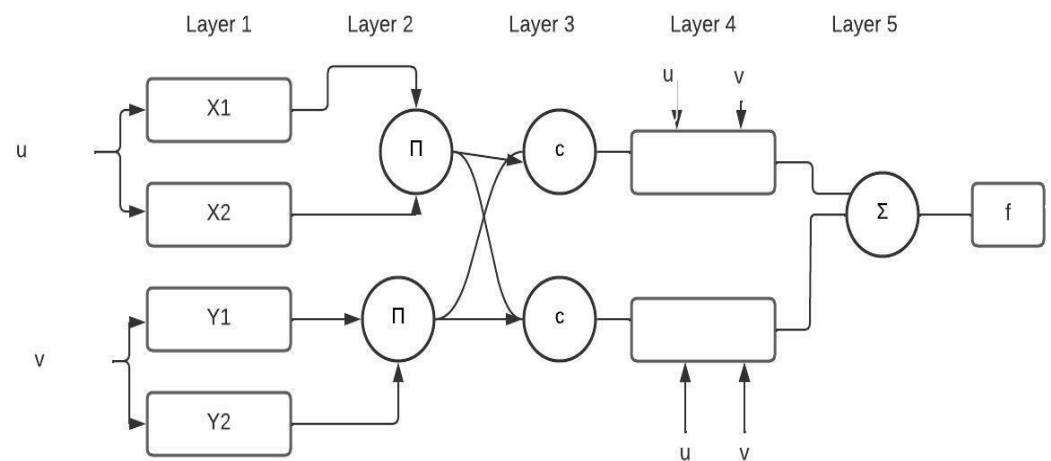


Figure 1. The architecture of ANFIS model.

2.2. Support Vector Machine (SVM)

Vapnik initially demonstrated the SVM in 1995. Researchers utilize this method to tackle categorization, prediction, and regression difficulties. It's a part of artificial intelligence (AI) [43,44]. SVM analysis involves training and testing data sets and input/output parameters. The optimal margin classifier is used in SVM analysis to segment the decision surface. The product of two vectors is determined using the kernel function approach. Fixed mapping is used to fit a non-linear kernel function in high-dimensional space after input data has been mapped using n -dimensional characteristics. When high-dimensional data is mapped using a kernel, the information separates linearly without altering the input space [44]. The input space is converted into a high-dimensional feature space via the kernel function, which enables non-linear relationships to be expressed in a linear fashion. The particular selection of a kernel function to map the non-linear input space into a linear feature space is highly dependent on the nature of the data, which refers to the type of underlying relationship that needs to be estimated in order to relate the input data with the desired output property. Finding such a kernel will be quite valuable. The Pearson VII Universal Kernel was utilized for use as the basis for the GP and SVM kernel function. The Pearson VII function offers outstanding flexibility and the opportunity to simply shift from a Gaussian into a Nonlinear peak shape and more by modifying its parameters. It also has the ability to transition from a Nonlinear peak shape to a Gaussian peak shape. As a result, the Pearson VII function can be utilized in place of a generic kernel [45].

2.3. Gaussian Processes (GPs)

Over the course of the last several years, a large amount of research and development effort has been concentrated on the study of machine learning as an area of study. The Gaussian process is a method for machine learning that involves performing analyses of models using kernels. It gives kernel machine novices hands-on experience [46,47]. Each finite random variable has a joint normal distribution. This collection is called a random variable ensemble. It is generally agreed that the mean function, which is represented by the symbol $m(x)$, and the kernel function, which is represented by the symbol $n(x, x')$, are the two most important functions of the Gaussian process, which is represented by the symbol $l(x)$.

2.4. Purpose of the Study

A comprehensive literature analysis found that fewer studies had utilized these modelling methodologies to assess the FS of concrete mixes including WMP. In civil engineering, their ability to predict the FS of concrete mixtures was evaluated using literature and lab data. In this paper, the effect of marble powder on flexural strength of concrete is demonstrated. Experimental investigations to study the effect of marble dust on flexural strength

exploring possible reasons for the gain in strength have been conducted. The study's goal is to assess the flexural strength of concrete that includes waste marble powder using machine learning methods, i.e., ANFIS, Support vector machines, and Gaussian processes approaches. Other algorithms were also tested on the dataset used for the study in addition to GP, SVM, and ANFIS, but they showed a poor coefficient of correlation value for the dataset. Therefore, in place of other conventional methodologies, ANFIS, support vector machine, and Gaussian process methods were used to predict the flexural strength of concrete.

In order to determine which modelling technique was the most effective at predicting the FS of concrete mix, the results were compared. This was done so that the most dependable modelling strategy could be selected. Flexural strength has also been studied by using the most reliable approach of sensitivity analysis in order to determine the influential independent variable to predict the dependent variable.

3. Methodology

In order to accomplish the goal of the study, which was to predict the FS of concrete, the following approach was taken: data was gathered on the FS of concrete, and various forms of soft computing were utilized. It was important to collect adequate data for the purpose of predicting the FS, and this was accomplished by carrying out experimental study and data from previously published studies.

3.1. Experimental Investigation

Each of the 120 beam specimens measuring 700 mm × 150 mm × 150 mm provided the following information regarding the testing materials and procedures:

3.1.1. Aggregate

CA with nominal diameters between 10 and 20 mm was incorporated in the concrete mixture. The particle size distribution of the aggregate was graded [48]. The SG, crushing, and impact were found to be 2.61, 23.67, and 6.74 percent, respectively, by ASTM C-128 and ASTM C-127 [49,50]. The mechanical characteristics of FA and CA are shown in Table 1.

Table 1. Mechanical Characteristics of Fine and Coarse Aggregates.

Experiment	Unit	Observed Value	Permissible Limit	Standard
Impact test of CA	%	6.74	<10	[50]
Crushing value of CA	%	23.67	>45	[50]
SG of CA	gm/cm ³	2.61	-	
Apparent SG of CA	gm/cm ³	2.82	-	[49]
WA of CA	%	2.82	-	
SG of FA	gm/cm ³	2.47	-	
Apparent SG of FA	gm/cm ³	2.51	-	[49]
WA of FA	%	0.6	-	

3.1.2. Cement

Cement according to ASTM C-150 [51] Type-I cement was utilized in this study. Table 2 lists the mechanical characteristics of cement.

Table 2. Mechanical Characteristics of cement.

Test	Unit	Value	Permissible Limit	Standard
Fineness	%	5.77	<10	[52]
Consistency	%	32	>45	[53]
Soundness	mm	3.33	<10	[54]
SG	gm/cm ³	3.1	-	[55]
Setting Time	min	Initial	40	-
		Final	360	-

3.1.3. Marble Powder

The Waste Marble Powder that was obtained came from its source, which was a marble company that was located locally. While Table 3 provides an explanation of the WMP's mechanical qualities, Figure 2 depicts the chemical analysis of the marble powder. An EDS analysis was carried out so that the elemental make-up of the WMP could be ascertained. The X-ray spectra, which can be seen in the image, are laid out with the energy, which is measured in keV, along the x-axis and the number of counts, which is measured along the y-axis. The information shown in Figure 2 makes it abundantly evident that Calcium and Oxygen have the highest weightage of all the elements.

Table 3. Mechanical Characteristics of MP.

Test	Unit	Value
Fineness	%	2.01
SG	gm/cm ³	2.44
Apparent SG	gm/cm ³	2.56
WA	%	1.96
Bulk SG	gm/cm ³	1.63

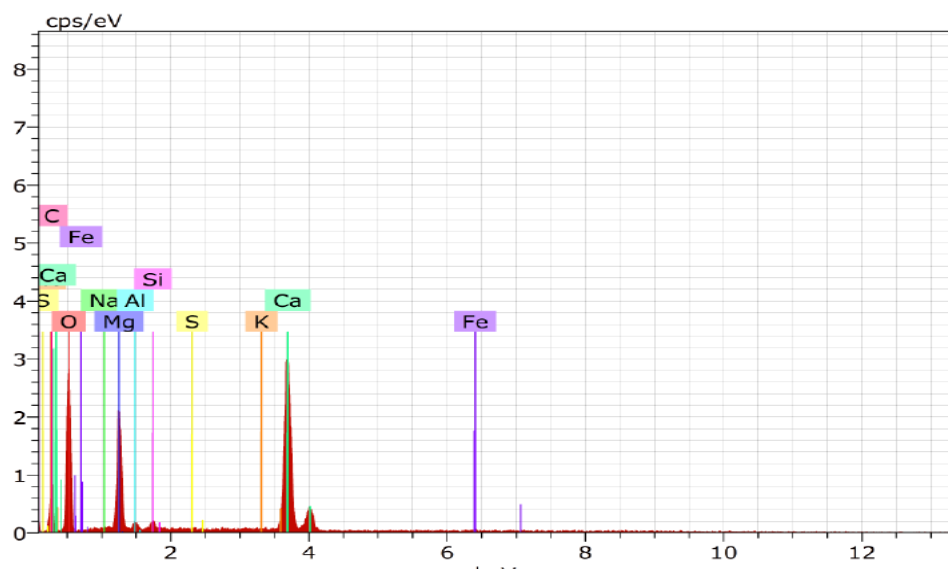


Figure 2. Chemical Analysis of Marble Powder.

3.1.4. Mix Design

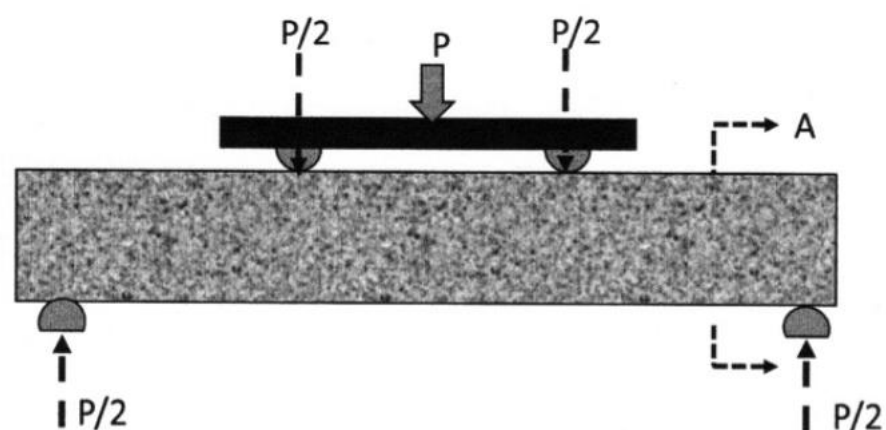
When making batches, the amounts of C, FA, and MP that were specified were employed. Other components, such as CA and the ratio of water to cement, were always used in the same proportions throughout the process. Several unique sets of specimens, each of which had three beams, were manufactured as a part of the experiment. A total of one hundred and twenty beams were manufactured. The composition of the control specimens, as well as the composition of the specimens with 5, 10, 15, and 20% replacement by the weight of cement and sand, is detailed in Table 4.

Table 4. Mix Design.

Sr. No.	Mix-ID	Materials in kg/m ³				
		Cement	FA	CA	Water	MP
1	M0	395.74	600.15	1103.09	217.65	0
2	A04	395.74	570.14	1103.09	217.65	30.00
3	A13	390.79	577.65	1103.09	214.93	27.44
4	A22	385.85	585.15	1103.09	212.21	24.89
5	A31	380.89	592.64	1103.09	209.49	22.34
6	A40	375.95	600.15	1103.09	206.77	19.78
7	B04	395.74	540.13	1103.09	217.65	60.01
8	B13	385.85	555.13	1103.09	212.21	54.90
9	B22	375.95	570.14	1103.09	206.77	49.75
10	B31	366.06	585.15	1103.09	201.33	44.68
11	B40	356.16	600.15	1103.09	195.89	39.57
12	C04	395.74	510.12	1103.09	217.65	90.02
13	C13	380.89	532.63	1103.09	209.49	82.35
14	C22	366.06	555.13	1103.09	201.33	74.69
15	C31	351.21	577.65	1103.09	193.16	67.02
16	C40	336.37	600.15	1103.09	185.00	59.36
17	D04	395.74	480.12	1103.09	217.65	120.03
18	D13	375.95	510.12	1103.09	206.77	109.80
19	D22	356.16	540.13	1103.09	195.89	99.58
20	D31	336.37	570.14	1103.09	185.00	89.43
21	D40	316.59	600.15	1103.09	174.12	79.14

M0 = control mix; (A represents 5% MP, B represents 10% MP, C represents 15% MP, D represents 20% MP) replacement.

ASTM D790 and ASTM C78 determine flexural strength using a two-point loading test. This method determines the flexural strength of hardened concrete test specimens by two-point loading [57,58]. Figure 3 shows a schematic of a flexural machine with two supports and two loads. Two supports considered as simply supported. The specimen's center was loaded and then two points until failure. The flexural test machine directly measured the load.

**Figure 3.** Experimental Setup for Flexural Strength [58].

3.1.5. Result and Discussion

The samples A04 and D40 that contained marble powder instead of sand and cement, respectively, showed an extra improvement in strength in the strength activity results as shown in Figure 4. After 28 days, the strength ratio for the samples was 15% and 3% higher, respectively, showing that a chemical reaction was occurring. The components with the

biggest weightage, according to an EDS study, are calcium and oxygen in marble powder, which contribute to the increase in strength.

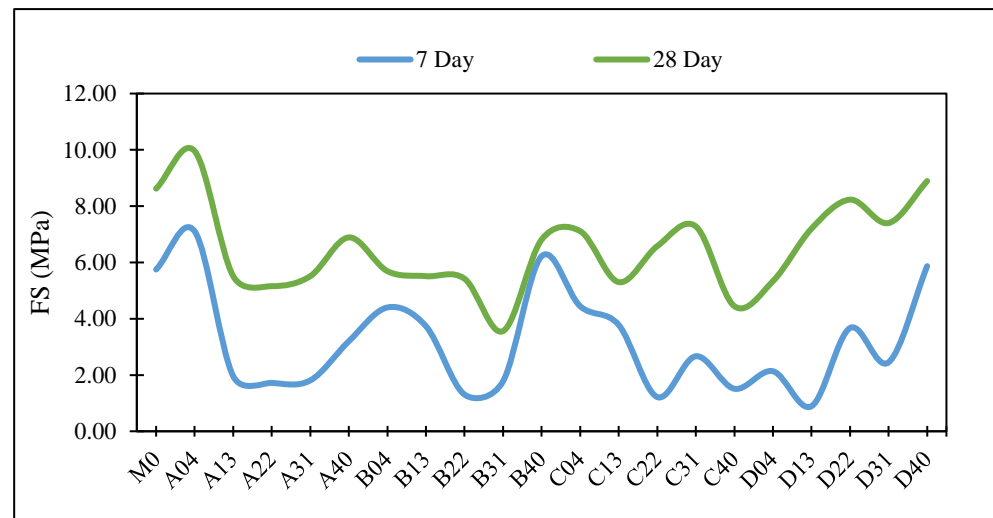


Figure 4. FS Results Based on Experimental Studies.

4. Statistical Analysis

4.1. Data Collection

The dataset is absolutely necessary for making an accurate prediction. Table 5 contains the range of the 202 observations that were gathered for this study from various sources, including the literature (82 readings), as well as laboratory data (120 readings). Table 6 contains detailed information regarding the observations that were analyzed as part of the investigation. After then, the 202 observations were divided into two subgroups at random, with a ratio of 70–30 for the training and testing subsets, respectively. In this study, FS served as the output variable, while ANFIS, SVM, and GP were the three methods that were employed to obtain the intended outcome. The input variables included C, FA, CA, w, MP, and CD. The software platforms that were used were MATLAB and Weka 3.9. In order to achieve the desired outcome, the researchers used independent variables including C, FA, CA, w, MP, and CD. In Table 7, the characteristics of the complete dataset, the dataset used for training, and the dataset used for testing are outlined. Consideration was given to the CC, MAE, RMSE, RAE, and RRSE when attempting to ascertain which model produced the most accurate results. These factors were helpful in determining which model was the most accurate. Better results are likely to have a higher CC value as well as a lower error value. Table 8 is a listing of the user-defined criteria that must be met when evaluating the FS of a concrete mixture using WMP. These user-defined optimal settings for various procedures are the product of a significant amount of research that were conducted. The effectiveness of each model was determined by the optimal configurations. Because the optimal parameters will have an effect on the performance of the model, it is essential that they be determined with extreme care. As a consequence of this, the example parameters were perfectly suitable for both the datasets used for training and for testing.

Table 5. Range of the dataset used.

Sr. No.	Independent Variable Range					CD	Dependent Variable Range		Reference
	(kg/m ³)						FS (MPa)		
	C	FA	CA	W	MP				
1.	316.59–395.74	480.12–600.15	1103.09	174.13–217.66	0.00–120.03	7.00–28.00	0.71–11.73	Experimental Reading	
2.	225.00–300.00	450.00	900.00	120.00	0.00–75.00	7.00–28.00	0.40–3.10	[59]	
3.	383.00	273.00–546.00	1187.00	191.60	0.00–273.00	28.00	4.18–5.73	[60]	
4.	340.00–400.00	672.00	1113.00	120.00–160.00	0.00–60.00	7.00–28.00	3.30–4.21	[61]	
5.	240.00–300.00	312.30	1721.40	150.000	0.00–30.00	7.00–90.00	4.80–6.10	[62]	
6.	270.20–337.80	741.40–927.00	1046.20	189.140–212.800	0.00–185.20	7.00–90.00	1.76–3.40	[63]	

Table 6. Detail of dataset.

Sr. No.	1	2	3	4	5	6	Total
Author	Mansoor [59]	Anitha Selvasofia [60]	Sounthararajan and Sivakumar [61]	Ergun [62]	Kirgiz [63]	Experimental Readings	202
No. of observation	18	6	14	22	22	120	

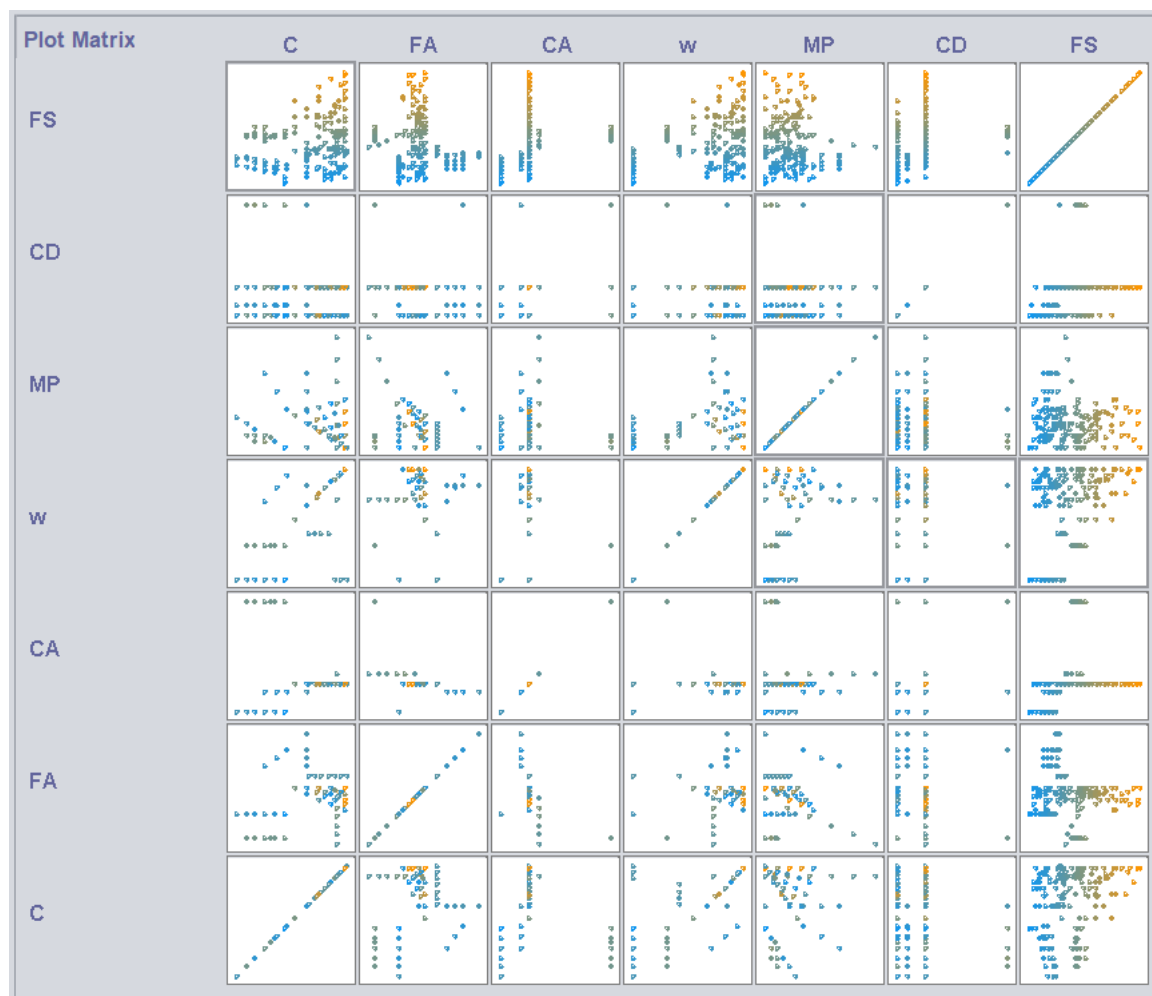
Table 7. Characteristics of Datasets.

Dataset	Statistics	Minimum	Maximum	Mean	Standard Deviation	Kurtosis	Skewness
Total Dataset (202 observations)	C	225.00	400.00	345.23	48.54	−0.43	−0.89
	FA	273.00	927.00	556.21	132.14	0.59	0.12
	CA	900.00	1721.40	1149.32	209.67	3.40	2.07
	w	120.00	217.66	186.23	31.89	−0.32	−1.01
	MP	0.00	273.00	59.71	46.51	2.48	1.29
	CD	7.00	90.00	20.10	16.64	8.33	2.44
	FS	0.40	11.73	4.55	2.52	0.01	0.67
Training Dataset (142 Observations)	C	225.00	400.00	343.55	50.30	−0.60	−0.82
	FA	273.00	927.00	554.14	137.09	0.53	0.15
	CA	900.00	1721.40	1155.17	218.49	2.80	1.96
	w	120.00	217.66	185.80	32.29	−0.45	−0.95
	MP	0.00	273.00	59.21	48.52	2.95	1.44
	CD	7.00	90.00	21.05	18.62	6.82	2.39
	FS	0.40	11.73	4.59	2.62	0.04	0.75
Testing Dataset (60 Observations)	C	225.00	395.74	349.21	44.23	0.14	−1.05
	FA	312.30	834.30	561.10	120.60	0.81	0.05
	CA	900.00	1721.40	1135.46	188.16	5.90	2.46
	w	120.00	217.66	187.26	31.15	0.13	−1.17
	MP	0.00	185.20	60.89	41.72	0.34	0.73
	CD	7.00	28.00	17.85	10.34	−2.02	−0.05
	FS	0.71	10.31	4.46	2.27	−0.44	0.32

Table 8. Use Defined Parameters.

Model Used	User Defined Parameters
SVM	C = 1.5, PUK kernel O = 0.7, S = 0.7
GP	Noise = 0.1, PUK kernel O = 0.8, S = 0.8
ANFIS	Epoches = 10

Figure 5, show how distinct each data point's colors are. The color alterations on the pair charts depend on the output's level of intensity. Figure 5 shows how the color for flexure strength, which ranges from 0.4 MPa to 11.73 MPa, varies from blue to orange depending on the intensity of the output. As a result, each data point's color is unique for each variable and ranges from blue at 0.4 MPa to orange at 11.73 MPa. In addition, Figure 5 illustrates a pair plot that was created to visualize the given dataset and discover their relationship. Figure 5 depicts the complex relationship that exists between the flexural strength of concrete and the constituent elements of marble powder, curing days, water, and cement. As can be seen, an increase in the dependent variables such as cement, water, marble powder, and curing days has an effect on the FS of the concrete.

**Figure 5.** Pair Plot of all Variables.

4.2. Criteria for Evaluative Assessment

Using evaluating parameters ensures that algorithms perform to their greatest capacity. The CC, MAE, RMSE, RAE, and RRSE were used in this investigation.

$$CC = \frac{x(\sum_{i=1}^x OV) - (\sum_{i=1}^x O)(\sum_{i=1}^x V)}{\sqrt{[x \sum_{i=1}^x O^2 - (\sum_{i=1}^x O)^2]} \sqrt{[x \sum_{i=1}^x V^2 - (\sum_{i=1}^x V)^2]}} \quad (1)$$

$$RMSE = \sqrt{\frac{1}{x} \left(\sum_{i=1}^x (V - O)^2 \right)} \quad (2)$$

$$MAE = \frac{1}{x} \left(\sum_{i=1}^x |V - O| \right) \quad (3)$$

$$RAE = \frac{\sum_{i=1}^x |O - V|}{\sum_{i=1}^x (|O - \bar{O}|)} \quad (4)$$

$$RRSE = \sqrt{\frac{\sum_{i=1}^x (O - V)^2}{\sum_{i=1}^x (|V - \bar{V}|)^2}} \quad (5)$$

O = Observed readings; \bar{O} = the average of the Observed readings

V = Predicted readings; \bar{V} = Predicted Values Average

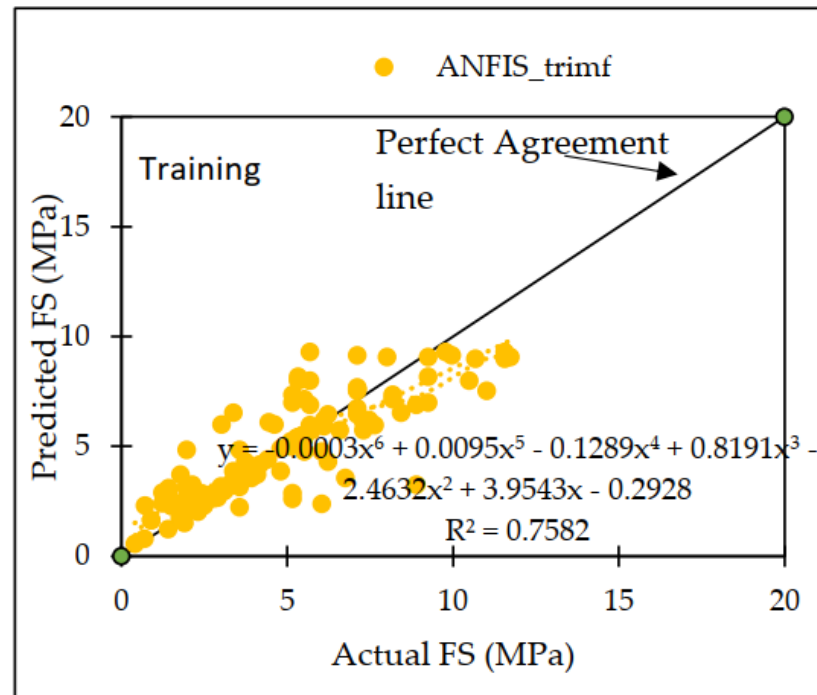
x = the total number of readings.

The numbers assigned to the CC might range from minus one to plus one. The higher the CC number, the more favorable the outcomes are projected to be. Lower values of evaluation parameters such as RMSE, MAE, RAE, and RRSE, on the other hand, predict better outcomes; that is, if the computed error is low, it means that the output results will be better [64–70].

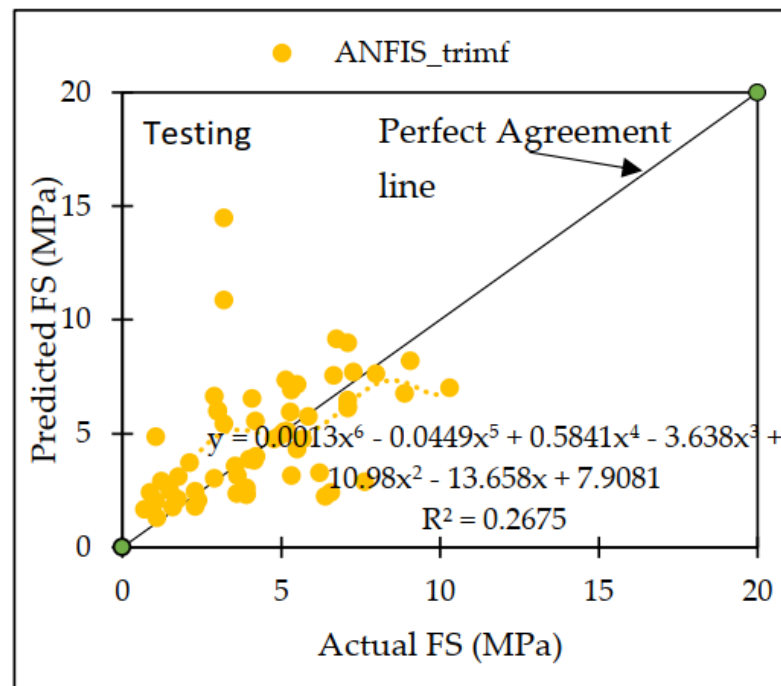
5. Findings and Discussion

5.1. ANFIS Based Assessment

Trial-and-error is used in the development of ANFIS-based models. Matlab can be used to predict FS. The model used in the study is triangular. The performance metrics for each membership function-based ANFIS model are listed in the later section. ANFIS model based on triangular membership function (MFs) predicts FS of concrete mix containing WMP. The CC values for training and testing were 0.8592 and 0.4687, respectively. The RMSE, MAE, RAE, and RRSE values were 1.3351 and 2.5116, 0.8487, 39.77% and 59.93%, respectively. Figure 6 illustrates observed and predicted ANFIS-based results for both phases. These numbers show how well the ANFIS trimf-based model predicts the FS of concrete mixes containing WMP. Reliable outcomes are predicted by a value that is closer to the line of perfect agreement [71–76].



(a) Training



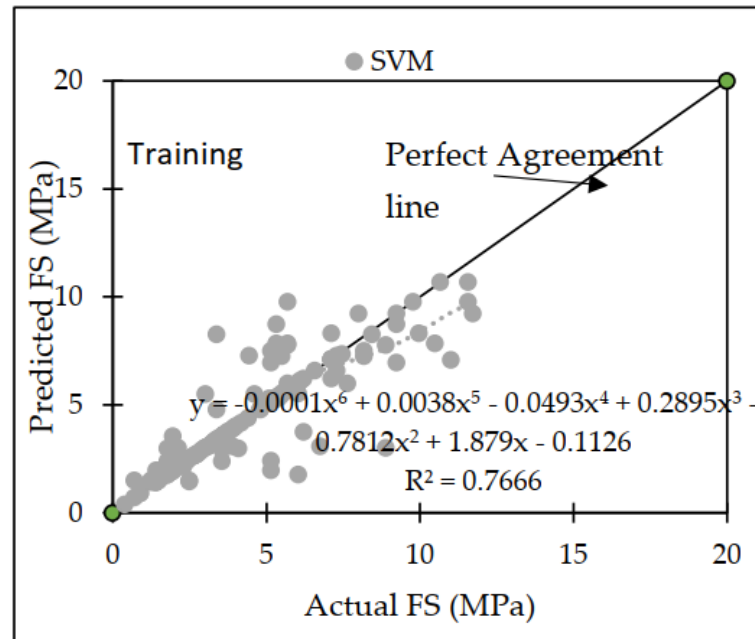
(b) Testing

Figure 6. The scatter graph shows observed and expected ANFIS FS values.

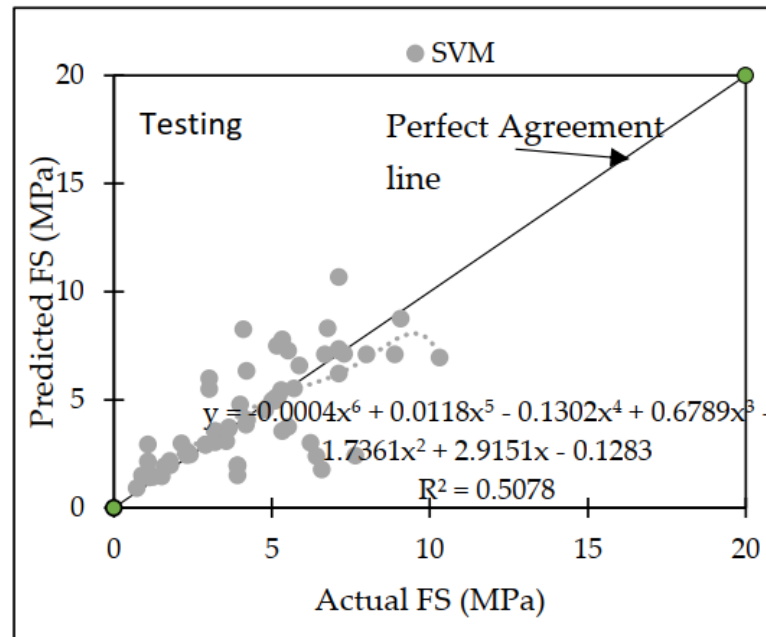
5.2. Support Vector Machine (SVM) Based Assessment

The Pearson VII function kernel, often known as the PUK kernel, is used in this model along with a number of user-defined parameters, such as C, omega (O), and sigma (S). The ideal method, which involved getting the maximum CC value while also minimizing the number of errors, was found after a substantial number of experiments were run [77–80]. The dataset that was used in this investigation yielded the most successful outcomes, with

a c value of 1.5, O = 0.7, and S = 0.7, respectively. The performance metrics of the SVM are listed in Table 9, and it includes both the training and testing datasets. The RRSE was 50.88 percent during the training phase and 78.36 percent during the testing phase. The RAE was 31.49 percent during the training phase and 61.61 percent during the testing phase. The MAE was 0.6720 during the training phase and 1.1604 during the testing phase. The CC values were 0.8656 and 0.7020. A comparison of the actual and anticipated FS values of the concrete mix resulted in the creation of the agreement plot, which is depicted in Figure 7.



(a) Training



(b) Testing

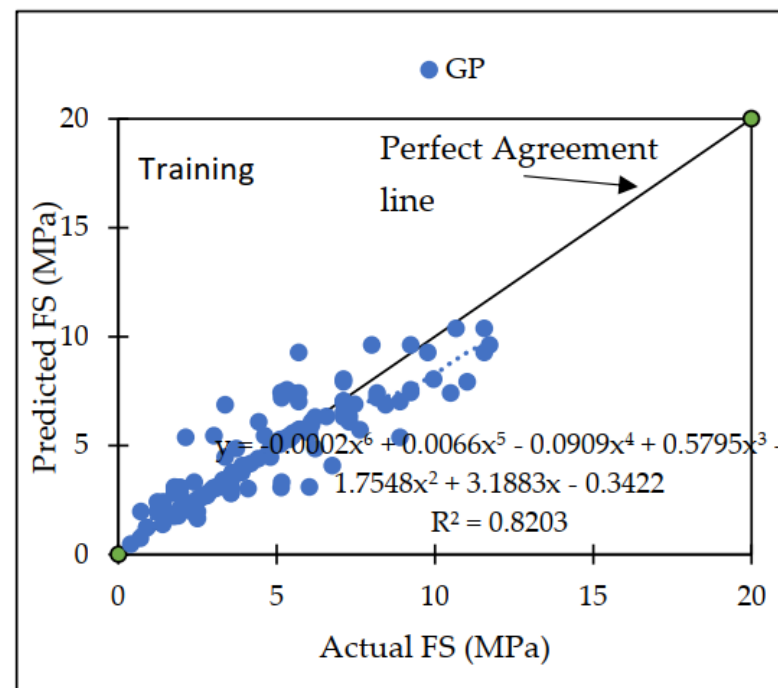
Figure 7. The scatter graph shows SVM-predicted and observed FS values.

Table 9. Performances of SVM, GP, and ANFIS.

Machine Learning Techniques	CC	MAE	RMSE	RAE	RRSE
Training					
GP	0.8967	0.7180	1.1563	33.64%	44.32%
SVM	0.8656	0.6720	1.3275	31.49%	50.88%
ANFIS_trimf	0.8592	0.8487	1.3351	39.77%	59.93%
Testing					
GP	0.7476	1.0884	1.5621	57.79%	69.19%
SVM	0.7020	1.1604	1.7691	61.61%	78.36%
ANFIS_trimf	0.4687	1.6305	2.5116	86.99%	98.74%

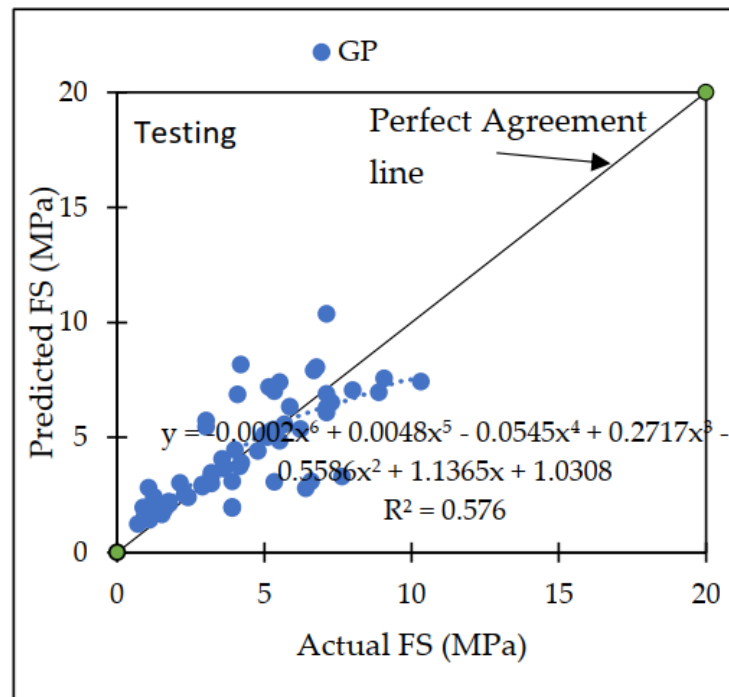
5.3. Gaussian Processes (GPs) Based Assessment

The type of regression known as Gaussian Processes makes use of a Pearson VII function kernel, often known as a PUK kernel, together with specific user-defined parameters such as L, Omega (O), and Sigma (S). Numerous trials had to be conducted in order to find the optimal value, which was defined as the greatest CC value that could be achieved with the fewest errors [81–84]. With L values of 0.1, O = 0.8, and S = 0.8, respectively, the dataset employed in this experiment yielded the most effective findings. Table 9 can be accessed here and contains the performance metrics for the general practice training and testing datasets. The training and testing phases' respective RMSE values were 1.1563 and 1.5621, the training and testing phases' respective MAE values were 0.7180 and 1.0884, the training and testing phases' respective RAE values were 33.64 percent and 57.79 percent, and the training and testing phases' respective RRSE values were 44.32 percent and 69.19 percent. The actual FS of the concrete mix is compared to the projected FS in Figure 8, which illustrates the agreement plot.



(a) Training

Figure 8. Cont.

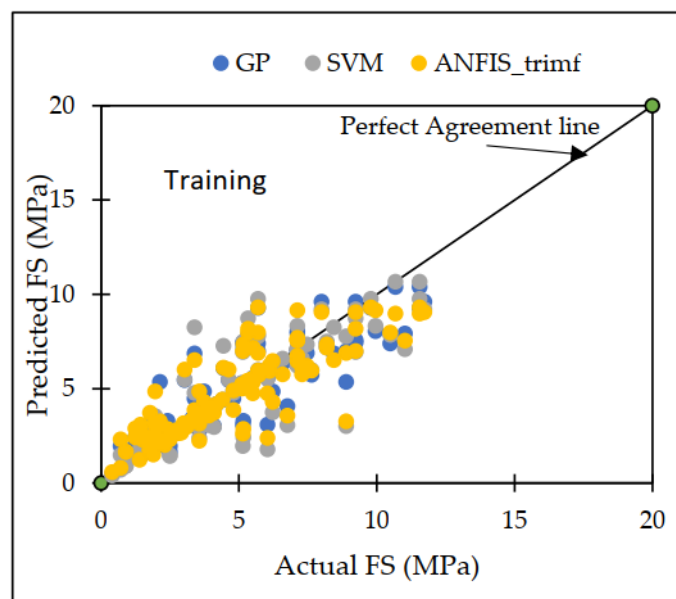


(b) Testing

Figure 8. The scatter graph displays the observed and GP-predicted FS.

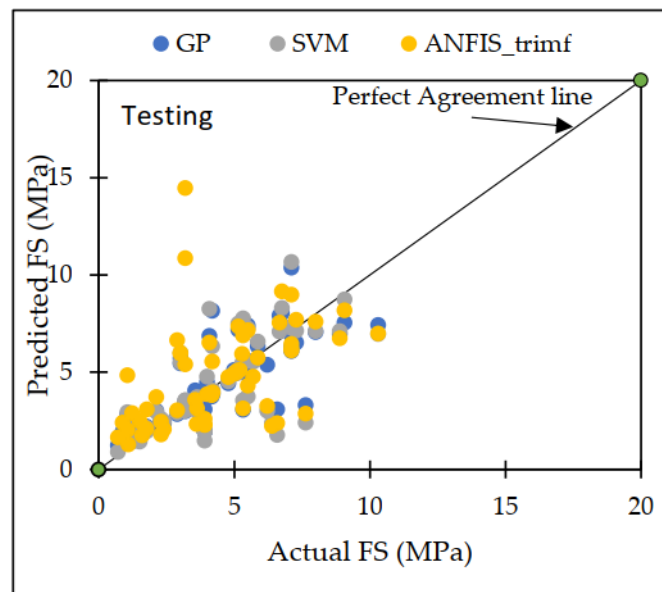
6. Comparison

Throughout the course of this investigation, a variety of distinct strategies for machine learning were utilized. The GP model appears to outperform the others when these models are compared, both in terms of the training datasets and the testing datasets [65]. Both the training dataset and the testing dataset showed that the GP model had the greatest possible CC values of 0.8967 and 0.7476, respectively, for the testing dataset. Figure 9a,b illustrates the disparity that exists between the projected dataset and the actual dataset on which machine learning methods were performed.



(a) Training

Figure 9. Cont.



(b) Testing

Figure 9. The scatter plot shows observed and predicted values of FS from SVM, GP, and ANFIS.

GP model also had the lowest MAE (1.0884), RMSE (1.5621), RAE (57.79%), and RRSE (69.19%) for the testing dataset. These results can be seen in Table 9 and Figure 10.

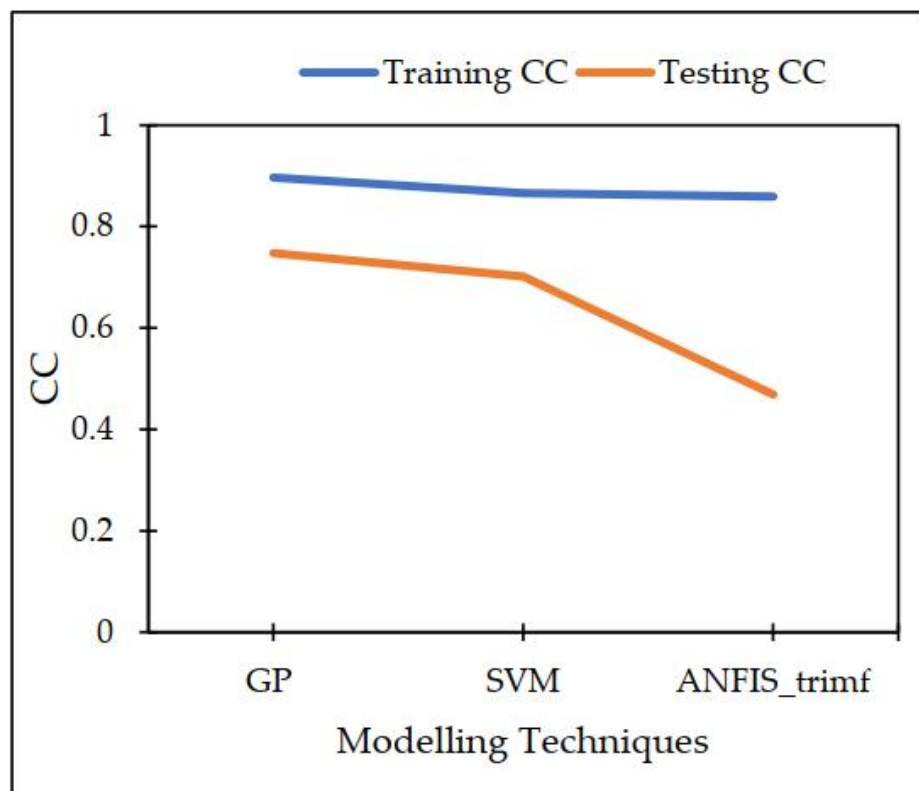


Figure 10. Cont.

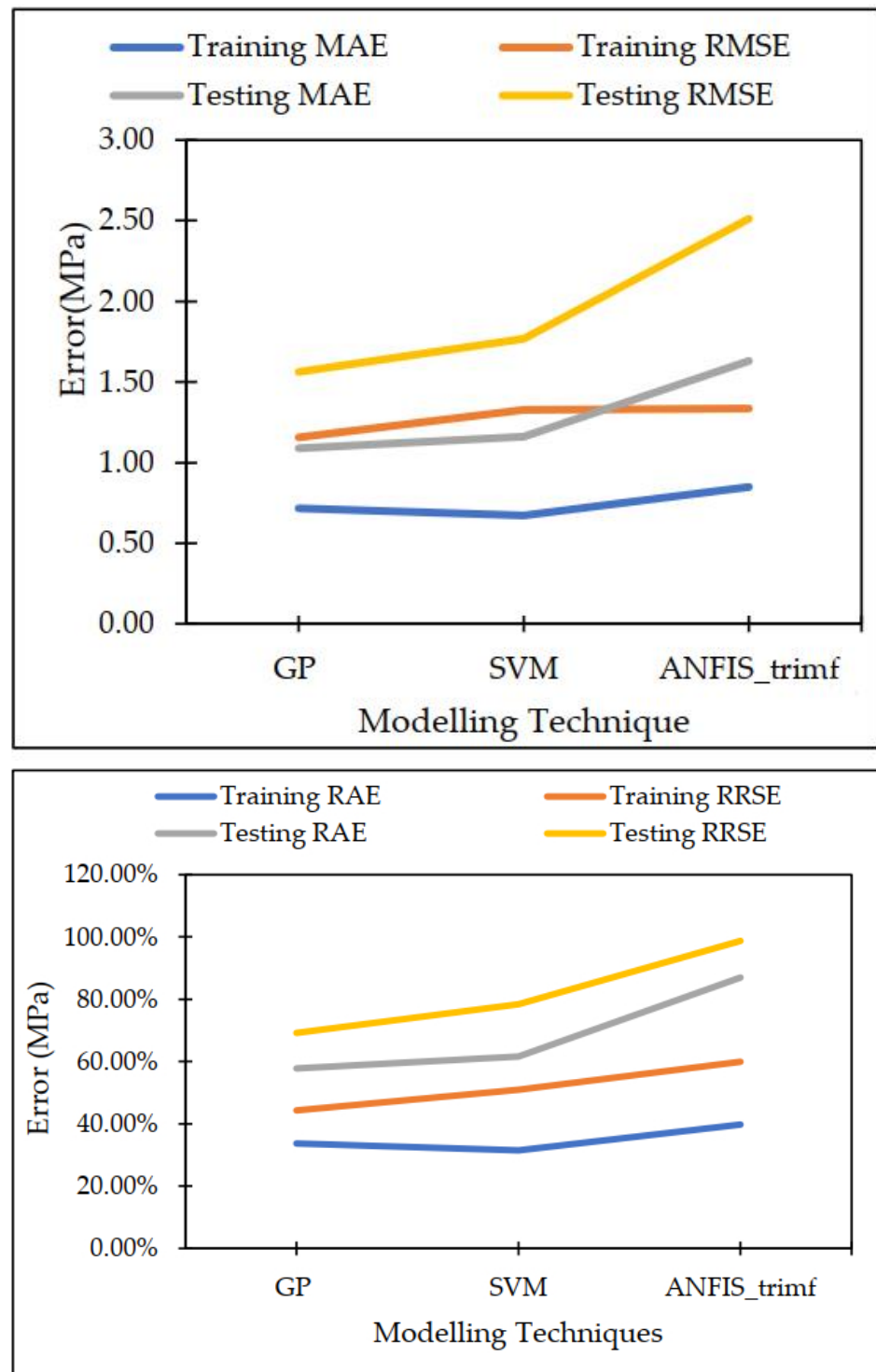
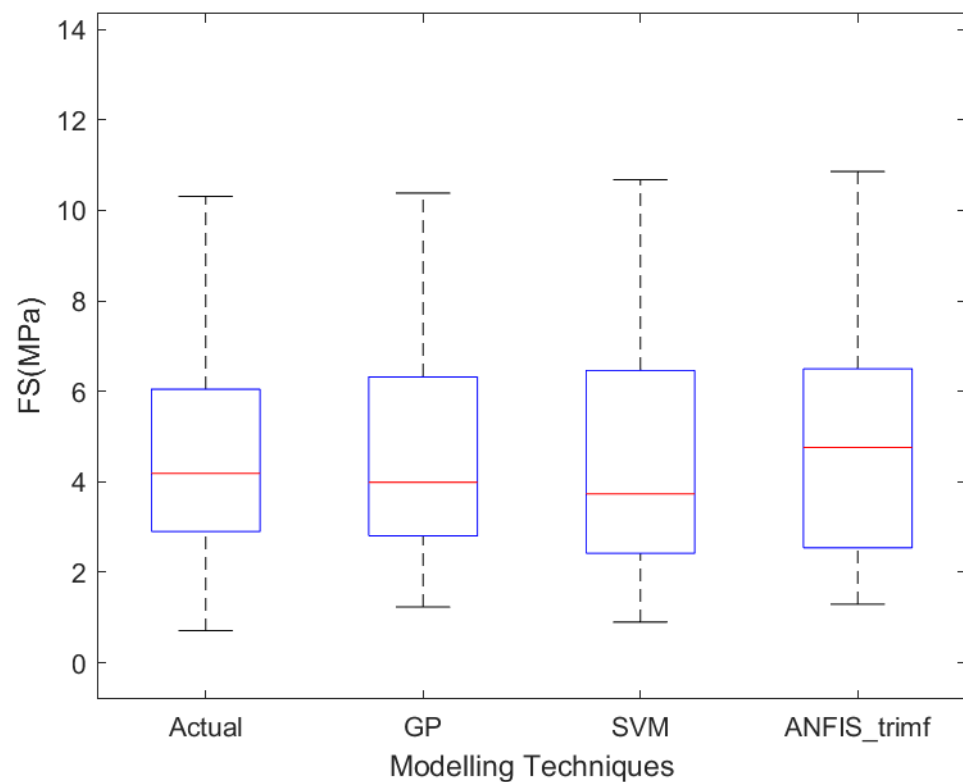


Figure 10. Performance Evaluation by Statistical Parameters.

In order to determine the FS of concrete mix that included MP, it was necessary to evaluate not only the actual value but also the quartile values of 25%, 50%, and 75% in addition to the actual value. Table 10 displays the findings obtained from the aforementioned assessments. Interquartile range (IQR) of GP is relatively near to IQR of the real data that was followed by ANFIS trimf, as can be shown in Figure 11 and Table 10, respectively.

Table 10. Statistics of observed and predicted output of testing dataset utilizing soft computing algorithms.

Output	Statistic Criteria	Actual	GP	SVM	ANFIS_Trimf
FS	Minimum	0.71	1.23	0.90	1.29
	Maximum	10.31	10.38	10.68	14.48
	1st Quartile	2.90	2.81	2.42	2.58
	Mean	4.46	4.50	4.41	4.83
	3rd Quartile	5.96	6.31	6.40	6.48
	IQR	3.06	3.50	3.98	3.90

**Figure 11.** Box plots for all Testing Dataset models.

In addition, based on the examination of the data, the set of data has been separated into two groups, which are $FS < 10$ MPa and $FS > 10$ MPa. Table 11 and Figure 12 show the increasing trend in error with decreasing FS based on the modelling methodologies that were used, and they indicate that the error increases from 0.6411 to 1.3511 MPa for $FS > 10$ to $FS < 10$, respectively, for GP based model.

Table 11. Performances of SVM, GP, and ANFIS for $FS < 10$ MPa and $FS > 10$ Mpa.

	MAE	
	GP	SVM
FS < 10	1.3511	1.6208
FS > 10	0.6411	0.6647

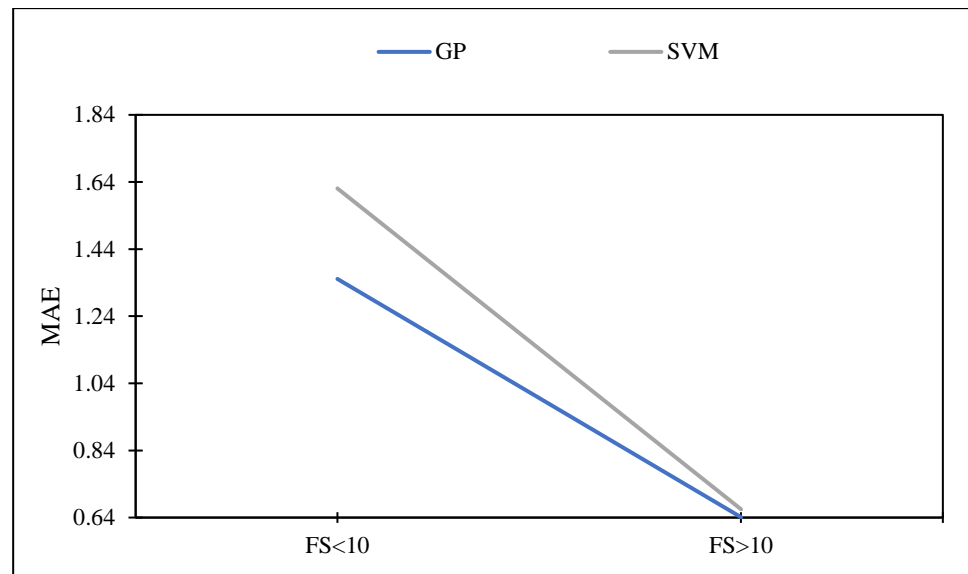


Figure 12. Relationship between Flexural Strength and MAE.

7. Sensitivity Assessments

The most important component of the input variable that affects the prediction of the FS of concrete mixes containing waste MP was identified as a possible variable using sensitivity analysis. It can be seen from Figure 4, which shows the experimental results, that curing days and the change in quantity of MP affects the concrete flexural strength of concrete. Further, sensitivity study was undertaken on the GP model because it performed the best among the other models for this dataset [85–87]. As shown in Table 12, this analysis involved changing the input combination and removing one input parameter one by one. For the purpose of determining which model performed the best, the study utilized statistical evaluation criteria such as CC, MAE, and RMSE. Table 12 indicates that one of the most important factors to consider when attempting to predict the FS of a concrete mixture is the number of curing days followed by the water. Figure 13 represents the relationship between removed parameter and the CC value based on the GP model. The following equation represents the best-fit model for independent variables:

$$y = -0.003x^5 + 0.0648x^4 - 0.5341x^3 + 2.0406x^2 - 3.4785x + 2.68 \quad (6)$$

where, x = independent variable, y = dependent variable

Table 12. GP-based sensitivity model results.

Removed Variable	GP Based Model		
	CC	MAE	RMSE
NIL (no parameter has been removed)	0.7713	1.2034	1.6713
CD	0.5441	1.5499	2.0857
w	0.7365	1.3137	1.8028
FA	0.7419	1.3177	1.7863
CA	0.7690	1.2135	1.6808
C	0.7641	1.2367	1.6909
MP	0.7774	1.1642	1.6194

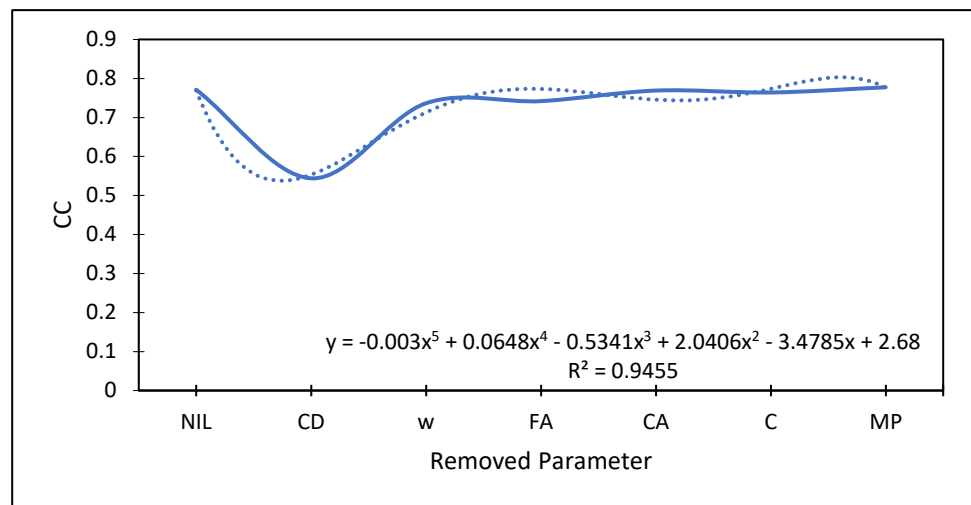


Figure 13. Relationship between Removed Parameters and CC Value Based on GP Model.

In addition, sensitivity analysis has been performed to check the sensitive variable when FS is divided into two parts, i.e., FS < 10 Mpa and FS > 10 Mpa. It can be seen from Table 13 that curing days has an influential effect on the flexural strength of the concrete with maximum MAE value, i.e., 4.8163 Mpa and 1.4743 Mpa for FS > 10 Mpa and FS < 10 Mpa, respectively. A gel is created during the pozzolanic reaction, which causes the FS to increase. Concrete can become stronger when the curing time is extended because it is a gradual process [66].

Table 13. GP-based sensitivity model results for FS < 10 and FS > 10.

Removed Variable	MAE	
	FS > 10	FS < 10
NIL (no parameter has been removed)	0.6411	1.3511
C	0.6378	1.0110
FA	0.6340	1.0131
CA	0.6411	0.9268
w	0.6379	1.0267
MP	0.6570	0.9492
CD	4.8163	1.4743

8. Conclusions

In this study, the algorithms that were used to predict the FS of concrete mixes that included WMP were compared using three different machine learning techniques. These techniques were ANFIS, SVM, and GP. The effectiveness of these models was assessed using the CC, MAE, RMSE, RAE, and RRSE metrics, respectively.

According to the results of the research, the GP model yields the most reliable predictions of the FS of concrete. This conclusion may be drawn from the data of the investigation. GP also predicts more accurate outcomes for the testing dataset than SVM, with corresponding CC values of 0.7476 and 0.7020, lower MAE values of 1.0884 and 1.1604, and lower RMSE values of 1.5621 and 1.7691, respectively.

The scatter plot demonstrates that the GP has the least error band width and is an important predictor of output. This is demonstrated by the fact that the GP has the smallest error band width. The amount of curing days that are subsequently followed by water is the most significant variable to take into consideration when attempting to estimate the FS of concrete. This is because, when compared to the other variables that are utilized as input for this data set, it is the most relevant variable.

Author Contributions: Conceptualization, N.S., M.A.M., A.A.A., M.A. and A.N.A.; methodology, N.S.; software, N.S.; validation, M.S.T.; formal analysis, N.S., M.A.M. and M.A.; investigation, N.S.; writing—original draft preparation, N.S.; writing—review and editing, M.S.T., M.A.M., A.A.A., M.A. and A.N.A.; visualization, N.S. and M.S.T.; Conceptualization, R.K.; methodology, R.K.; software, R.K., M.A.M., A.A.A., M.A. and A.N.A.; validation, R.K., formal analysis, investigation, R.K. All authors have read and agreed to the published version of the manuscript.

Funding: The authors acknowledge the support of Prince Sultan University for paying the article processing charges (APC) of this publication.

Institutional Review Board Statement: Not applicable.

Informed Consent Statement: Not applicable.

Data Availability Statement: Not applicable.

Acknowledgments: The authors would like to acknowledge the support received by Taif University Researchers Supporting Project number (TURSP-2020/240), Taif University, Taif, Saudi Arabia.

Conflicts of Interest: The authors declare no conflict of interest.

Abbreviations

CA	Coarse aggregate
CC	Coefficient of correlation
CS	Compressive strength
CD	Curing days
FA	Fine aggregate
FS	Flexural strength
GP	Gaussian Process
GMDH	Group method of data handling
MP	Marble powder
MAE	Mean absolute error
RAE	Relative absolute error
RMSE	Root mean squared error
RRSE	Root relative squared error
SG	Specific Gravity
SVM	Support vector machine
w	Water
WMP	Waste marble powder
WA	Water absorption

References

1. Eliche-Quesada, D.; Corpas-Iglesias, F.A.; Perez-Villarejo, L.; Iglesias-Godino, F.J. Recycling of sawdust, spent earth from oil filtration, compost and marble residues for brick manufacturing. *Constr. Build. Mater.* **2012**, *34*, 275–284. [[CrossRef](#)]
2. Cui, Y.; Liu, J.; Wang, L.; Liu, R.; Pang, B. A model to characterize the effect of particle size of fly ash on the mechanical properties of concrete by the grey multiple linear regression. *Comput. Concr.* **2020**, *26*, 175–183. [[CrossRef](#)]
3. Belaidi, A.S.E.; Azzouz, L.; Kadri, E.; Kenai, S. Effect of natural pozzolana and marble powder on the properties of self-compacting concrete. *Constr. Build. Mater.* **2012**, *31*, 251–257. [[CrossRef](#)]
4. Ghani, A.; Ali, Z.; Khan, F.A.; Shah, S.R.; Khan, S.W.; Rashid, M. Experimental study on the behavior of waste marble powder as partial replacement of sand in concrete. *SN Appl. Sci.* **2020**, *2*, 1554. [[CrossRef](#)]
5. Ashish, D.K.; Verma, S.K.; Kumar, R.; Sharma, N. Properties of concrete incorporating sand and cement with waste marble powder. *Adv. Concr. Constr.* **2016**, *4*, 145–160. [[CrossRef](#)]
6. Sharma, N.; Thakur, M.S.; Goel, P.L.; Sihag, P. A review: Sustainable compressive strength properties of concrete mix with replacement by marble powder. *J. Achiev. Mater. Manuf. Eng.* **2020**, *98*, 11–23. [[CrossRef](#)]
7. Agarwal, S.K.; Gulati, D. Utilization of industrial wastes and unprocessed micro-fillers for making cost effective mortars. *Constr. Build. Mater.* **2006**, *20*, 999–1004. [[CrossRef](#)]
8. Ahmed, K.; Nizami, S.; Raza, N.; Mahmood, K. Effect of micro sized marble sludge on physical properties of natural rubber composites. *Chem. Ind. Chem. Eng.* **2013**, *19*, 281–293. [[CrossRef](#)]
9. Soliman, N.M. Effect of using marble powder in concrete mixes on the behavior and strength. *Int. J. Curr. Eng. Technol.* **2013**, *3*, 1863–1870.

10. Shirule, P.A.; Rahman, A.; Gupta, R.D. Partial replacement of cement with marble. *Int. J. Adv. Eng. Res. Stud.* **2012**, *30*, 175–177.
11. Dhoka, M.C. Green Concrete: Using industrial waste of marble powder, quarry dust and paper pulp. *Int. J. Eng. Sci. Invent.* **2013**, *2*, 67–70.
12. Vaidevi, C. Engineering study on marble dust as partial replacement of cement in concrete. *Indian J. Eng.* **2013**, *4*, 14–16.
13. Aruntas, H.Y.; Guru, M.; Dayi, M.; Tekin, I. Utilization of waste marble dust as an additive in cement production. *Mater. Des.* **2010**, *31*, 4039–4042. [[CrossRef](#)]
14. Kelestemur, O.; Arici, E.; Yildiz, S.; Gokcer, B. Performance evaluation of cement mortars containing marble dust and glass fiber exposed to high temperature by using taguchi method. *Constr. Build. Mater.* **2014**, *60*, 17–24. [[CrossRef](#)]
15. Topcu, I.B.; Bilir, T.; Uygunoglu, T. Effect of waste marble dust content as filler on properties of self-compacting concrete. *Constr. Build. Mater.* **2009**, *23*, 1947–1953. [[CrossRef](#)]
16. Ashish, D.K. Feasibility of waste marble powder in concrete as partial substitution of cement and sand amalgam for sustainable growth. *J. Build. Eng.* **2017**, *15*, 236–242. [[CrossRef](#)]
17. Uysal, M.; Yilmaz, K. Effect of mineral admixtures on properties of self-compacting concrete. *Cem. Concr. Compos.* **2011**, *33*, 771–776. [[CrossRef](#)]
18. Hebhoub, H.; Aoun, H.; Belachia, M.; Houari, H.; Ghorbel, E. Use of waste marble aggregates in concrete. *Constr. Build. Mater.* **2011**, *25*, 1167–1171. [[CrossRef](#)]
19. Corinaldesi, V.; Moriconi, G.; Naik, T.R. Characterization of marble powder for its use in mortar and concrete. *Constr. Build. Mater.* **2010**, *24*, 113–117. [[CrossRef](#)]
20. Uysal, M.; Sumer, M. Performance of self-compacting concrete containing different mineral admixtures. *Constr. Build. Mater.* **2011**, *25*, 4112–4120. [[CrossRef](#)]
21. Demirel, B. The effect of using waste marble dust as fine sand on the mechanical properties of the concrete. *Int. J. Phys. Sci.* **2010**, *5*, 1372–1380.
22. Elyamany, H.E.; Abd Elmoaty, A.E.M.; Mohamed, B. Effect of filler types on physical, mechanical and microstructure of self compacting concrete and flow-able concrete. *Alex. Eng. J.* **2014**, *53*, 295–307. [[CrossRef](#)]
23. Sharma, N.; Thakur, M.S.; Upadhyaya, A.; Sihag, P. Evaluating flexural strength of concrete with steel fibre by using machine learning techniques. *Compos. Mater. Eng.* **2021**, *3*, 201–220. [[CrossRef](#)]
24. Thakur, M.S.; Pandhiani, S.M.; Kashyap, V.; Upadhyaya, A.; Sihag, P. Predicting Bond Strength of FRP Bars in Concrete Using Soft Computing Techniques. *Arab. J. Sci. Eng.* **2021**, *46*, 4951–4969. [[CrossRef](#)]
25. Sobhani, J.; Najimi, M.; Pourkhorshidi, A.R.; Parhizkar, T. Prediction of the compressive strength of no-slump concrete: A comparative study of regression, neural network and ANFIS models. *Constr. Build. Mater.* **2010**, *24*, 709–718. [[CrossRef](#)]
26. Sharma, N.; Upadhyaya, A.; Thakur, M.S.; Sihag, P. Comparison of Machine learning algorithms to evaluate Strength of Concrete with Marble Powder. *Adv. Mater. Res.* **2022**, *11*, 75–90. [[CrossRef](#)]
27. Sharma, N.; Thakur, M.S.; Sihag, P.; Malik, M.A.; Kumar, R.; Abbas, M.; Saleel, C.A. Machine learning techniques for evaluating concrete strength with waste marble powder. *Materials* **2022**, *15*, 5811. [[CrossRef](#)]
28. Yaswanth, K.K.; Revathy, J.; Gajalakshmi, P. Artificial intelligence for the compressive strength prediction of novel ductile geopolymer composites. *Comput. Concr.* **2021**, *28*, 55–68. [[CrossRef](#)]
29. Gholamzadeh-Chitgar, A.; Berenjian, J. Elman ANNs along with two different sets of inputs for predicting the properties of SCCs. *Comput. Concr.* **2019**, *24*, 399–412. [[CrossRef](#)]
30. Biswas, R.; Bardhan, A.; Samui, P.; Rai, B.; Nayak, S.; Armaghani, D.J. Efficient soft computing techniques for the prediction of compressive strength of geopolymer concrete. *Comput. Concr.* **2021**, *28*, 221–232. [[CrossRef](#)]
31. Kumar, A.; Rupali, S. Prediction of UCS and STS of Kaolin clay stabilized with supplementary cementitious material using ANN and MLR. *Adv. Comput. Des.* **2019**, *5*, 195–207. [[CrossRef](#)]
32. Chore, H.S.; Magar, R.B. Prediction of unconfined compressive and Brazilian tensile strength of fiber reinforced cement stabilized fly ash mixes using multiple linear regression and artificial neural network. *Adv. Comput. Des.* **2017**, *2*, 225–240. [[CrossRef](#)]
33. Sharma, N.; Thakur, M.S.; Upadhyaya, A.; Sihag, P. Evaluation of models by soft computing techniques for the prediction of compressive strength of concrete using steel fibre. In *Applications of Computational Intelligence in Concrete Technology*; CRC Press: Boca Raton, FL, USA, 2022. [[CrossRef](#)]
34. Poddar, A.; Kumar, A.; Kashyap, V.; Thapa, S. Data-driven modeling approach in model rainfall-runoff for a mountainous catchment. In *Modeling and Simulation of Environmental Systems*; CRC Press: Boca Raton, FL, USA, 2022; pp. 253–268.
35. Kashyap, V.; Poddar, A.; Kumar, N.; Rustum, R. A Comparative Study Using ANFIS and ANN for Determining the Compressive Strength of Concrete. In *Applications of Computational Intelligence in Concrete Technology*; CRC Press: Boca Raton, FL, USA, 2022; pp. 73–91.
36. Alyaseen, A.; Poddar, A.; Alissa, J.; Alahmad, H.; Almohammed, F. Behavior of CFRP-strengthened RC beams with web openings in shear zones: Numerical simulation. *Mater. Today Proc.* **2022**, *65*, 3229–3239. [[CrossRef](#)]
37. Alyaseen, A.; Poddar, A.; Almohammed, F.; Tajjour, S.; Hammadeh, K.; Alahmad, H. Compressive strength prediction and analysis of concrete using hybrid artificial neural networks. In *Applications of Computational Intelligence in Concrete Technology*; CRC Press: Boca Raton, FL, USA, 2022; pp. 285–303.

38. Alyaseen, A.; Poddar, A.; Almohammed, F.; Tajjour, S.; Hammadeh, K.; Alahmad, H. Predicting recycled aggregates compressive strength in high-performance concrete using artificial neural networks. In *Applications of Computational Intelligence in Concrete Technology*; CRC Press: Boca Raton, FL, USA, 2022; pp. 269–283.
39. Madandoust, R.; John, H.B.; Reza, G. Prediction of the concrete compressive strength by means of core testing using GMDH-type neural network and ANFIS models. *Comput. Mater. Sci.* **2012**, *51*, 261–272. [[CrossRef](#)]
40. Ayat, H.; Kellouche, Y.; Ghrici, M.; Boukhatem, B. Compressive strength prediction of limestone filler concrete using artificial neural networks. *Adv. Comput. Des.* **2018**, *3*, 289–302. [[CrossRef](#)]
41. Upadhya, A.; Thakur, M.S.; Sharma, N.; Sihag, P. Assessment of Soft Computing-Based Techniques for the Prediction of Marshall Stability of Asphalt Concrete Reinforced with Glass Fiber. *Int. J. Pavement Res. Technol.* **2021**, *15*, 1366–1385. [[CrossRef](#)]
42. Kumar, S.; Dhanabalan, S.; Narayanan, C.S. Application of ANFIS and GRA for multi-objective optimization of optimal wire-EDM parameters while machining Ti–6Al–4V alloy. *SN Appl. Sci.* **2019**, *1*, 298. [[CrossRef](#)]
43. Salcedo-Sanz, S.; Rojo-Alvarez, J.L.; Martinez-Ramon, M.; Camps-Valls, G. Support vector machines in engineering: An overview. *WIREs Data Min. Knowl. Discov.* **2014**, *4*, 234–267. [[CrossRef](#)]
44. Goh, A.T.C.; Goh, S.H. Support vector machines: Their use in geotechnical engineering as illustrated using seismic liquefaction data. *Comput. Geotech.* **2007**, *34*, 410–421. [[CrossRef](#)]
45. Abakar, K.A.A.; Yu, C. Performance of SVM based on PUK kernel in comparison to SVM based on RBF kernel in prediction of yarn tenacity. *Indian J. Fibre Text. Res.* **2014**, *39*, 55–59.
46. Rasmussen, C.E.; Williams, C.K.I. *Gaussian Processes for Machine Learning*; The MIT Press: Cambridge, MA, USA, 2006.
47. Deepa, C.; Sathiyakumari, K.; Preamsudha, V. Prediction of the compressive strength of high-performance concrete mix using tree based modeling. *Int. J. Comput. Appl.* **2010**, *6*, 18–24. [[CrossRef](#)]
48. *ASTM D6913-04*; Standard Test Methods for Particle Size Distribution of Soils. American Society for Testing of Materials: West Conshohocken, PA, USA, 1992.
49. *ASTM C-128*; Standard Test Method for Specific Gravity and Absorption of Fine Aggregate. Annual Book of ASTM Standards: West Conshohocken, PA, USA, 1992.
50. *ASTM C 127*; Test Method for Specific Gravity and Adsorption of Coarse Aggregate. Annual Book of ASTM Standards: West Conshohocken, PA, USA, 1992.
51. *ASTM C150/C150M-21*; Standard Specification for Portland Cement. ASTM International: West Conshohocken, PA, USA, 2021.
52. *ASTM C184-94e1*; Standard Test Method for Fineness of Hydraulic Cement by the 150- μ m (No. 100) and 75- μ m (No. 200) Sieves (Withdrawn 2002). ASTM International: West Conshohocken, PA, USA, 1994.
53. *ASTM C187-16*; Standard Test Method for Amount of Water Required for Normal Consistency of Hydraulic Cement Paste. ASTM International: West Conshohocken, PA, USA, 2016.
54. *ASTM C151/C151M-18*; Standard Test Method for Autoclave Expansion of Hydraulic Cement. ASTM International: West Conshohocken, PA, USA, 2018.
55. *ASTM C188-17*; Standard Test Method for Density of Hydraulic Cement. American Society for Testing and Material: West Conshohocken, PA, USA, 2009.
56. *ASTM C191-19*; Standard Test Methods for Time of Setting of Hydraulic Cement by Vicat Needle. ASTM International: West Conshohocken, PA, USA, 2019.
57. *ASTM D790-10*; Standard Test Methods for Flexural Properties of Unreinforced and Reinforced Plastics and Electrical Insulation Materials. ASTM International: West Conshohocken, PA, USA, 2007.
58. *ASTM C78-10*; ASTM International. Standard Test Method for Flexural Strength of Concrete (Using Simple Beam with Third-Point Loading). ASTM International: West Conshohocken, PA, USA, 2010.
59. Mansoor, J.; Shah, S.A.R.; Khan, M.M.; Sadiq, A.N.; Anwar, M.K.; Siddiq, M.U.; Ahmad, H. Analysis of mechanical properties of self-compacted concrete by partial replacement of cement with industrial wastes under elevated temperature. *Appl. Sci.* **2018**, *8*, 364. [[CrossRef](#)]
60. Anitha-Selvasofia, S.D.; Dinesh, A.; Sarath-Babu, V. Investigation of waste marble powder in the development of sustainable concrete. *Mater. Today Proc.* **2021**, *44*, 4223–4226. [[CrossRef](#)]
61. Sounthararajan, V.M.; Sivakumar, A. Effect of the lime content in marble powder for Producing high strength concrete. *J. Eng. Appl. Sci.* **2013**, *8*, 260–264.
62. Ergun, A. Effects of the usage of diatomite and waste marble powder as partial replacement of cement on the mechanical properties of concrete. *Constr. Build. Mater.* **2011**, *25*, 806–812. [[CrossRef](#)]
63. Kirgiz, M.S. Fresh and hardened properties of green binder concrete containing marble powder and brick powder. *Eur. J. Environ. Civ. Eng.* **2016**, *20*, 64–101. [[CrossRef](#)]
64. Nhu, V.H.; Shahabi, H.; Nohani, E.; Shirzadi, A.; Ansari, N.A.; Bahrami, S.; Miraki, S.; Geertsema, M.; Nguyen, H. Daily water level prediction of zrebar lake (Iran): A Comparison between M5P, Random Forest, Random Tree and Reduced Error Pruning Trees Algorithms. *Int. J. Geo-Inf.* **2020**, *9*, 479. [[CrossRef](#)]
65. Hoang, N.D.; Pham, A.D.; Nguyen, Q.L.; Pham, Q.N. Estimating compressive strength of high-performance concrete with gaussian process regression model. *Adv. Civ. Eng.* **2016**, *2016*, 2861380. [[CrossRef](#)]
66. Suthar, M. Applying several machine learning approaches for the prediction of unconfined compressive strength of stabilized pond ashes. *Neural Comput. Appl.* **2019**, *32*, 9019–9028. [[CrossRef](#)]

67. Afzal, A.; Khan, S.A.; Islam, T.; Jilte, R.D.; Khan, A.; Soudagar, M.E.M. Investigation and Back-Propagation Modeling of Base Pressure at Sonic and Supersonic Mach Numbers. *Phys. Fluids* **2020**, *32*, 096109. [[CrossRef](#)]
68. David, O.; Okwu, M.O.; Oyejide, O.J.; Taghinezhad, E.; Asif, A.; Kaveh, M. Optimizing Biodiesel Production from Abundant Waste Oils through Empirical Method and Grey Wolf Optimizer. *Fuel* **2020**, *281*, 118701. [[CrossRef](#)]
69. Afzal, A.; Saleel, C.A.; Badruddin, I.A.; Khan, T.M.Y.; Kamangar, S.; Mallick, Z.; Samuel, O.D.; Soudagar, M.E.M. Human Thermal Comfort in Passenger Vehicles Using an Organic Phase Change Material—An Experimental Investigation, Neural Network Modelling, and Optimization. *Buold. Environ.* **2020**, *180*, 107012. [[CrossRef](#)]
70. Afzal, A.; Alshahrani, S.; ASobaihan, A.; Buradi, A.; Khan, S.A. Power Plant Energy Predictions Based on Thermal Factors Using Ridge and Support Vector Regressor Algorithms. *Energies* **2021**, *14*, 7254. [[CrossRef](#)]
71. Afzal, A. Optimization of Thermal Management in Modern Electric Vehicle Battery Cells Employing Genetic Algorithm. *J. Heat Transf.* **2021**, *143*, 112902. [[CrossRef](#)]
72. Afzal, A.; Navid, K.M.Y.; Saidur, R.; Razak, R.K.A.; Subbiah, R. Back Propagation Modeling of Shear Stress and Viscosity of Aqueous Ionic—MXene Nanofluids. *J. Therm. Anal. Calorim.* **2021**, *145*, 2129–2149. [[CrossRef](#)]
73. Mokashi, I.; Afzal, A.; Khan, S.A.; Abdullah, N.A.; Bin Azami, M.H.; Jilte, R.D.; Samuel, O.D. Nusselt Number Analysis from a Battery Pack Cooled by Different Fluids and Multiple Back-Propagation Modelling Using Feed-Forward Networks. *Int. J. Therm. Sci.* **2021**, *161*, 106738. [[CrossRef](#)]
74. Elumalai, P.V.; Krishna Moorthy, R.; Parthasarathy, M.; Samuel, O.D.; Owamah, H.I.; Saleel, C.A.; Enweremadu, C.C.; Sreenivasa Reddy, M.; Afzal, A. Artificial Neural Networks Model for Predicting the Behavior of Different Injection Pressure Characteristics Powered by Blend of Biofuel-Nano Emulsion. *Energy Sci. Eng.* **2022**, *10*, 2367–2396. [[CrossRef](#)]
75. Veza, I.; Afzal, A.; Mujtaba, M.A.; Tuan Hoang, A.; Balasubramanian, D.; Sekar, M.; Fattah, I.M.R.; Soudagar, M.E.M.; EL-Seesy, A.I.; Djamari, D.W.; et al. Review of Artificial Neural Networks for Gasoline, Diesel and Homogeneous Charge Compression Ignition Engine: Review of ANN for Gasoline, Diesel and HCCI Engine. *Alex. Eng. J.* **2022**, *61*, 8363–8391. [[CrossRef](#)]
76. Bakır, H.; Ağbulut, Ü.; Gürel, A.E.; Yıldız, G.; Güvenç, U.; Soudagar, M.E.M.; Hoang, A.T.; Deepanraj, B.; Saini, G.; Afzal, A. Forecasting of Future Greenhouse Gas Emission Trajectory for India Using Energy and Economic Indexes with Various Metaheuristic Algorithms. *J. Clean. Prod.* **2022**, *360*, 131946. [[CrossRef](#)]
77. Sharma, P.; Said, Z.; Kumar, A.; Nižetić, S.; Pandey, A.; Hoang, A.T.; Huang, Z.; Afzal, A.; Li, C.; Le, A.T.; et al. Recent Advances in Machine Learning Research for Nanofluid-Based Heat Transfer in Renewable Energy System. *Energy Fuels* **2022**, *36*, 6626–6658. [[CrossRef](#)]
78. Sharma, J.; Soni, S.; Paliwal, P.; Saboor, S.; Chaurasiya, P.K.; Sharifpur, M.; Khalilpoor, N.; Afzal, A. A Novel Long Term Solar Photovoltaic Power Forecasting Approach Using LSTM with Nadam Optimizer: A Case Study of India. *Energy Sci. Eng.* **2022**, *10*, 2909–2929. [[CrossRef](#)]
79. Ziaee, O.; Zolfaghari, N.; Baghani, M.; Baniassadi, M.; Wang, K. A modified cellular automaton model for simulating ion dynamics in a Li-ion battery electrode. *Energy Equip. Syst.* **2022**, *10*, 41–49.
80. Taslimi, M.S.; Maleki Dastjerdi, S.; Bashiri Mousavi, S.; Ahmadi, P.; Ashjaee, M. Assessment and multi-objective optimization of an off-grid solar based energy system for a Conex. *Energy Equip. Syst.* **2021**, *9*, 127–143.
81. Sharifi, M.; Amidpour, M.; Mollaei, S. Investigating carbon emission abatement long-term plan with the aim of energy system modeling; case study of Iran. *Energy Equip. Syst.* **2018**, *6*, 337–349.
82. Zare, S.; Ayati, M.; Ha'iri Yazdi, M.R.; Kabir, A.A. Convolutional neural networks for wind turbine gearbox health monitoring. *Energy Equip. Syst.* **2022**, *10*, 73–82.
83. Sabzi, S.; Asadi, M.; Moghbelli, H. Review, analysis and simulation of different structures for hybrid electrical energy storages. *Energy Equip. Syst.* **2017**, *5*, 115–129.
84. Meignanamoorthy, M.; Ravichandran, M.; Mohanavel, V.; Afzal, A.; Sathish, T.; Alamri, S.; Khan, S.A.; Saleel, C.A. Microstructure, mechanical properties, and corrosion behavior of boron carbide reinforced aluminum alloy (al-Fe-Si-Zn-Cu) matrix composites produced via powder metallurgy route. *Materials* **2021**, *14*, 4315. [[CrossRef](#)]
85. Sathish, T.; Mohanavel, V.; Ansari, K.; Saravanan, R.; Karthick, A.; Afzal, A.; Alamri, S.; Saleel, C.A. Synthesis and characterization of mechanical properties and wire cut EDM process parameters analysis in AZ61 magnesium alloy+ B4C+ SiC. *Materials* **2021**, *14*, 3689. [[CrossRef](#)]
86. Chairman, C.A.; Ravichandran, M.; Mohanavel, V.; Sathish, T.; Rashedi, A.; Alarifi, I.M.; Badruddin, I.A.; Anqi, A.E.; Afzal, A. Mechanical and abrasive wear performance of titanium di-oxide filled woven glass fibre reinforced polymer composites by using taguchi and edas approach. *Materials* **2021**, *14*, 5257. [[CrossRef](#)]
87. Nagaraja, S.; Kodandappa, R.; Ansari, K.; Kuruniyan, M.S.; Afzal, A.; Kaladgi, A.R.; Aslfattahi, N.; Saleel, C.A.; Gowda, A.C.; Bindiganavile Anand, P. Influence of heat treatment and reinforcements on tensile characteristics of aluminium aa 5083/silicon carbide/fly ash composites. *Materials* **2021**, *14*, 5261. [[CrossRef](#)]